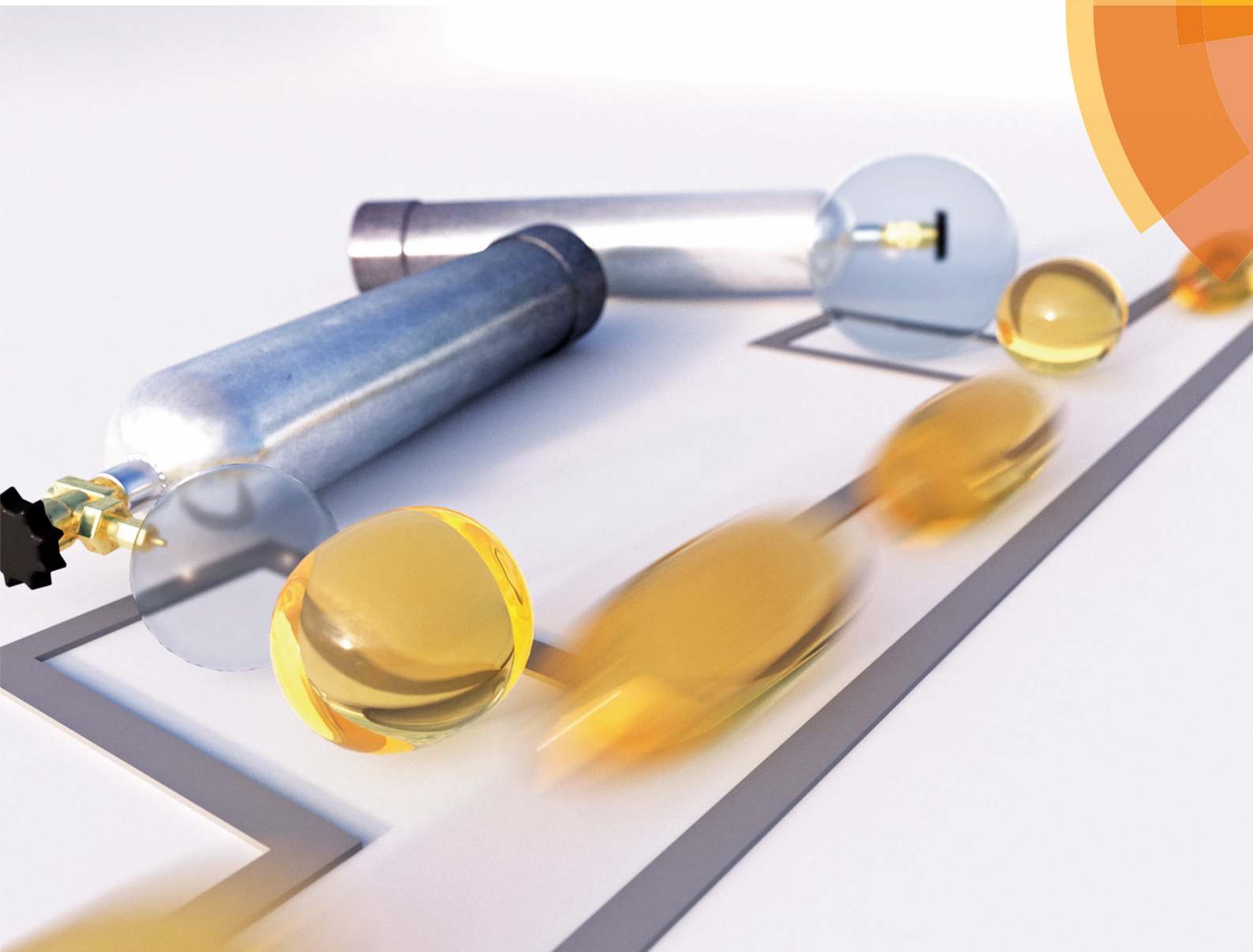# Analyst

PAPER
Richard W. Rambach, Preetika Biswas, Ashutosh Yadav, Piotr Garstecki and
Thomas Franke
Fast selective trapping and release of picoliter droplets in a 3D microfluidic
PDMS multi-trap system with bubbles

Fast selective trapping and release of picoliter droplets in a 3D microfluidic PDMS multi-trap system with bubbles

Richard W. Rambach,[a] Preetika Biswas,[a,b] Ashutosh Yadav,[a,b] Piotr Garstecki [ID][c] and Thomas Franke [ID] *[a,b]

The selective manipulation and incubation of individual picoliter drops in high-throughput droplet based microfluidic devices still remains challenging. We used a surface acoustic wave (SAW) to induce a bubble in a 3D designed multi-trap polydimethylsiloxane (PDMS) device to manipulate multiple droplets and demonstrate the selection, incubation and on-demand release of aqueous droplets from a continuous oil flow. By controlling the position of the acoustic actuation, individual droplets are addressed and selectively released from a droplet stream of 460 drops per s. A complete trapping and releasing cycle can be as short as 70 ms and has no upper limit for incubation time. We characterize the fluidic function of the hybrid device in terms of electric power, pulse duration and acoustic path.

Introduction

Droplets are a powerful tool in microfluidics due to their ability to act as small sample containers.[1] They provide closed entities and are used to encapsulate bacteria, cells, biochemical solutes and other reactants of interest. They are extremely versatile and have been used in a myriad of different applications from cell sorting, drug discovery[2] and delivery,[3] high-throughput screening,[4] and directed evolution of cells and enzymes[5] to protein crystallization.[6] Droplets provide several advantages over conventional techniques. It is possible to generate and work with a large number of droplets,[7] they can hold ultra-small volumes and it is possible to operate complex fluidic handling protocols automatically.[8,9] The metering, splitting, merging and moderating of the speed of a single droplet has been impressively demonstrated.[10–12]

Yet, most of the microfluidic devices developed have focussed on the analysis of droplets in arrays (*i.e.* in batches),[13–22] while others operate on single drops one by one in series.[23–28] One important feature of droplet manipulation in series is the capture and immobilization of individual droplets, which remains challenging. Existing approaches have

been able to capture single droplets[13–19,29] and cells[30] but the selection of individual droplets/particles in these studies is random. In contrast, the controlled trapping of individual droplets has been shown using small groves in the channel but the system involves only a very small flow or droplet rate[10,31] (*e.g.* 10 μl h⁻¹ for the dispersed phase resulting in about 30 drops per s). The release of trapped droplets has been achieved by flowing an excess continuous phase of oil or by reversing the flow of the trapped droplets.[10,14–16,29,32] In a trapping system for giant unilamellar vesicles (GUVs) the continuous phase has to be increased over a critical value for releasing the trapped GUVs,[33] which is quite similar to another publication.[34] To overcome these limitations, other studies have been made. A system has been shown that is able to trap and release single cancer cells and particles with a hydrodynamic and pressure driven actuation system (one valve per trap), yet with a rather slow performance (*e.g.* several seconds for loading)[35] Very recently, two devices, using surface acoustic waves, have also been demonstrated, yet they similarly suffer from a slow performance and low droplet rate[36,37] (about 2–3 drops per s). While controlled trapping and fusion of droplets have been demonstrated using high-voltage electric fields,[38,39] these approaches require charged interfaces, a condition that limits their range of applications and is potentially harmful for biological samples. A general method for the controlled trapping and release of multiple picoliter droplets at the microfluidic scale and at high speed has not been shown.

Here we demonstrate the use of surface acoustic waves (SAWs) for the controlled fast trapping, incubation and release of individually selected droplets from a continuously flowing

[a] Soft Matter and Biological Physics Group, Universität Augsburg, Universitätsstr. 1, D-86159 Augsburg, Germany

[b] Division of Biomedical Engineering, School of Engineering, University of Glasgow, Oakfield Avenue, G12 8LT Glasgow, UK. E-mail: Thomas.Franke@glasgow.ac.uk

[c] Institute of Physical Chemistry, Polish Academy of Sciences, Kasprzaka 44/52, 01-224 Warsaw, Poland. E-mail: garst@ichf.edu.pl

stream with a high rate of 460 drops per s. The system allows us to manipulate individual droplets on demand without disturbing the flow of other droplets or altering the density, temperature or size of the droplets. Each drop can be individually addressed, manipulated and released by selecting the appropriate operation frequency of the SAW and can be incubated for variable incubation times as required.

Fabrication and experimental setup

An SU-8 (negative photoresist) 3D structure on a silicon wafer is produced by photolithography to act as a mask for the fabrication of a multilayer PDMS microchannel by soft lithography. A first SU-8 layer of 15 μm thickness is spin coated on a silicon wafer, soft baked, exposed to the mask of the first layer and hard baked. It is then coated with a second layer of SU-8 (15 μm) and soft baked. The mask of the second layer is then aligned with the exposed structures of the first layer and exposure is done followed by hard baking and spin coating of SU-8 (15 μm) for the third layer. The third layer is produced aligning the mask for the third layer with the structures of the second layer as described above. After the hard baking, the SU-8 structure is developed using MR-Dev 600 (Micro Resist Technology GmbH). The final structure fabricated is shown in Fig. 1.

The PDMS microchannel produced was bonded with a thin PDMS foil coated on a SU-8 coated Si wafer using O_2 plasma, to seal the open channels.

A tapered interdigital transducer (TIDT) with an aperture of 500 μm, a wavelength from 23 to 24.3 μm and 60 finger pairs was used to generate surface acoustic waves (SAWs). It was produced by depositing 100 nm of aluminium on a $LiNbO_3$ (128° y-cut) substrate (17.5 mm × 17.5 mm) with an adhesive layer in between $LiNbO_3$ and aluminium. A frequency generator (SML-01, Rhode & Schwartz) was connected to the IDT along with an amplifier (ZHL-1-2W, Mini Circuits) in between.

The PDMS microchannel was mounted onto the IDT chip and connected to two micro-syringe pumps (PHD2000, Harvard apparatus). The two pumps injected deionised water (dispersive phase) and oil (3M Novec 7500 Engineered Fluid, continuous phase), respectively. The water was stained with Patent Blue (1 mg ml^{-1}), and a surfactant (fluorosurfactant ammonium carboxylate, DuPoint Krytox 157) was added to the oil at a concentration of 0.5 wt%. The setup was observed under an optical microscope (CKX41, Olympus, Germany), and a high speed camera (FASTCAM 1024 PCI, Photron) was used to record the trapping of droplets. For all the results, a flow rate of 350 μl h^{-1} (continuous phase) and 75 μl h^{-1} (dispersive phase) was used. The drop rate of the averaged 45 pl droplets

Fig. 1 A: Micrograph of the multiple trap design. The multi-trap arrangement has five traps (marked as 1–5 in different colours) arranged from left to right. The picoliter droplets enter the channel from the left and proceed towards the exit at the right. The interdigitated transducer (IDT) is placed at the bottom and can be used to generate surface acoustic waves (SAW) in the y-direction hitting the coupling channels (marked yellow). The traps are connected to coupling channels *via* restrictions (marked red). B: Profilometer measurement of the 3D trapping design. The microchannel is a multiple layer design. It is fabricated by three consecutive photolithographic processes on three separate 15 μm SU-8 photoresist layers. This is done to achieve different heights for different parts of the trap, necessary for the proper functioning of the setup. The channels that carry the droplets are 30 μm in height, the traps are 45 μm in height and the restrictions along with intercoupling channel connections are 15 μm in height each.

was determined to be 460 drops per s and can be calculated using:

$$\text{Droplet rate} = \frac{Q_{\text{dispersive}}}{V_{\text{droplet}}}. \quad (1)$$

Experiment and results

The multilayer PDMS device is placed on a piezoelectric substrate (lithium niobate) with the produced IDT. The water and the oil flow intersect at the T-junction, where droplets of water are created in the continuous phase of oil. The droplet emulsion flows into the microchannel system from the left side (see Fig. 1), where they pass by the traps without entering them. The traps are loaded on demand by a single acoustic pulse. The droplets in the channels are on average 30 μm in width, 50 μm in length and 30 μm in height. They are in a squeezed shape in the channels as the channel walls prevent a spherical

shape. The microchannel system consists of the main channel (30 μm height) where the droplets are travelling, the traps (45 μm height) and the coupling channels (30 μm height) connected by small restriction shunts (15 μm height). As the restrictions have only a height of 15 μm, any trapped droplet would have to considerably deform in order to escape the trap though the restrictions. Thus, the high Laplace pressure required for deformation prevents droplets from squeezing through the restrictions.

The frequency generator applies a desired RF signal to the LiNbO$_3$ crystal using the aluminium fingers. The LiNbO$_3$ crystal will vibrate due to the inverse piezoelectric effect and if the spacing between the fingers is half of the wavelength of the RF signal, constructive interference occurs generating a SAW which propagates in the *y*-direction. The orientation of the LiNbO$_3$ (128° y-cut) guarantees that mainly Rayleigh waves are excited.

The transducer is a tapered IDT (also named slanted IDT), *i.e.* the spacing between the fingers changes linearly over the aperture. This allows the IDT to be actuated at different spots along the *x*-direction using different frequencies.

In the initial state, droplets pass by the traps and all traps are empty. By the application of a long SAW pulse (350 ms) in the middle of the PDMS channels (between traps 3 and 4) a bubble is generated, as shown in Fig. 2. When the SAW is turned off at a user defined time (point in time is independent of the positions of the drops), the bubble retreats and droplets enter the traps. All traps are loaded with a single droplet each. The traps being 45 μm in height (in comparison with the 30 μm height of the main channel) provide a room for the droplets to expand and the trapped droplets become spherical in shape. The droplets can be stored in the traps for several minutes.

They were then released by on-demand actuation as shown in Fig. 3. With different frequencies the position of the acoustic path can be controlled (compare Fig. 4). Depending on


Fig. 2 SAW induced trapping of droplets. (A) No droplet enters the trap when no SAW is applied. (B) A SAW pulse at a specific position, controlled by the applied frequency, is injected. The SAW hits the coupling channel and a bubble is generated at this location. (C) When the SAW is shut off, the bubble collapses and droplets (marked blue) are loaded into the traps. Successive droplets are passing by the already loaded traps. A pulse length of 350 ms and a pulse power of 29 dBm were used.
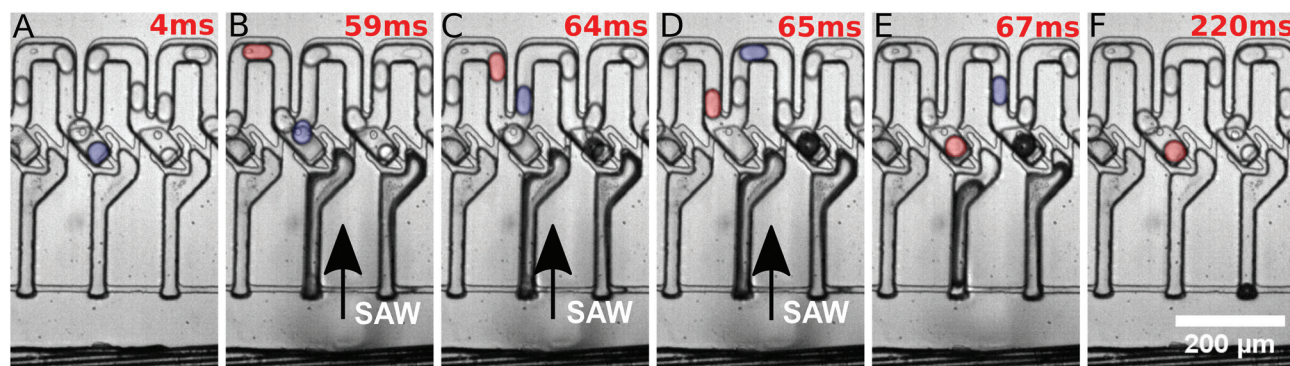
Fig. 3 Selective release of a trapped droplet and automatic refilling. (A) Multiple traps are loaded with droplets and subsequent droplets pass by the traps. No SAW is applied. (B & C) The SAW is locally applied (marked by arrow) and induces a bubble in the coupling channel. It pushes the oil in the channel towards the trap, forcing the droplet (marked blue) to move out of the trap. The SAW generates also a bubble right next to the actuated trap, but this bubble is less pronounced and thus not able to push out the droplet in the appropriate trap. (D) Another droplet (marked red) approaches towards the trap and (E) enters the trap when the SAW is turned off. (F) The droplet remains in the trap as long as no SAW is applied. A pulse length of 57 ms and a pulse power of 29 dBm were used.
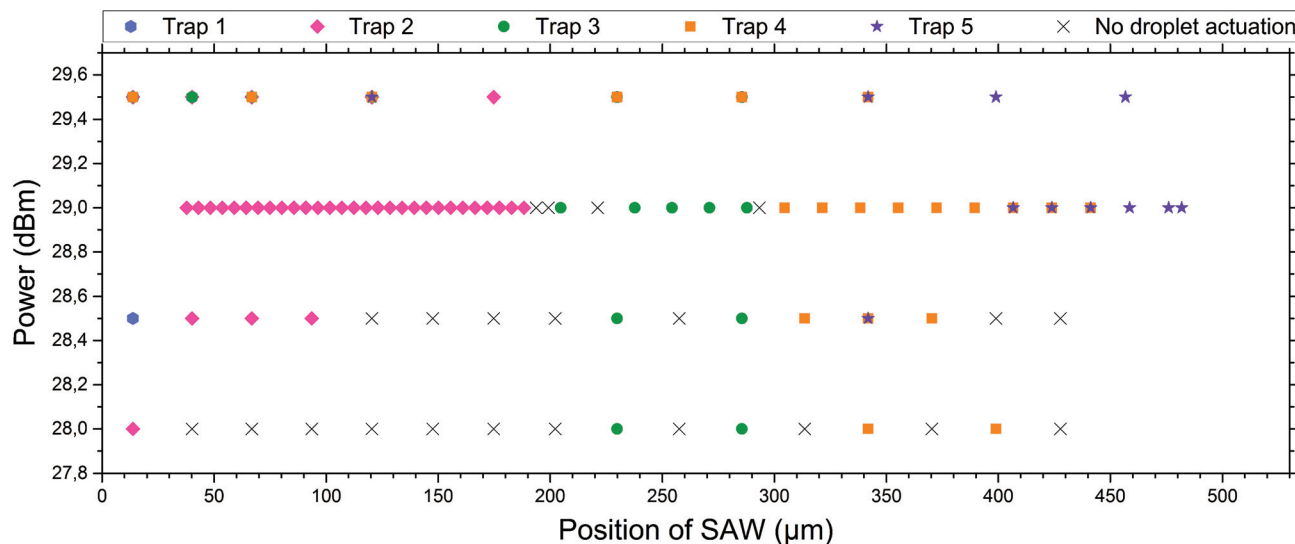
Fig. 4 Droplet release in dependence of power and position of the SAW. For different positions (the result of different applied frequencies) the SAW hits the coupling channels of the microfluidic system at different spots and consequently different traps (marked by colours, see the inserted label and compare with Fig. 1) are actuated. The actuation was performed using different powers of SAW. At powers below 29 dBm, not all droplets can be pushed out of the appropriate traps and there are positions where no droplet can be actuated (black crosses). Above 29 dBm multiple traps are actuated by a single SAW pulse and a selective release of single droplets is not possible. At 29 dBm selective release of individual droplets is possible. The first trap cannot be actuated properly during this specific experimental setup, as the IDT was slightly shifted to the right of the microfluidic system, and therefore an actuation of the very left trap was not possible. The errors in the measurements, corresponding to the error of the frequency generator for power and frequency, were very small and thus neglected in the graph. A pulse length of 350 ms was used.

where the SAW hits the coupling channel, the bubble is generated at different locations. It actuates the appropriate trap pushing out the droplet inside the trap. It is then immediately refilled by a subsequent droplet (see Fig. 3).

Different powers are used to actuate the droplets in the traps. For powers below 28 dBm, actuation was not possible. For powers of 28 dBm and 28.5 dBm different traps can be actuated and individual droplets can be released, but actuating trap 5 was not possible. For a power of 29 dBm, all traps can be selectively activated and the system is very robust. For a power of 29.5 dBm the traps could be actuated, but not each individually. A single SAW pulse at a distinct position releases two droplets, each of a different trap. The result has been summarised in Fig. 4. It shows the power *vs.* the position of the traps where the SAW is applied.

The minimum time needed to actuate the traps was measured for different powers. The results are summarised in Fig. 5. The data were measured for the third trap and it was found that the trap could be actuated with a small pulse length of 57 ms with a power of 29 dBm. At lower powers, the pulse length needed for pushing a droplet out of the third trap increases.

Discussion and conclusions

The applied technique of SAWs is an established practice in the field of microfluidics, and several applications have already been demonstrated[40–42] like fluid mixing,[43,44] fluid translation,[45–48] jetting and atomization,[49,50] particle, droplet
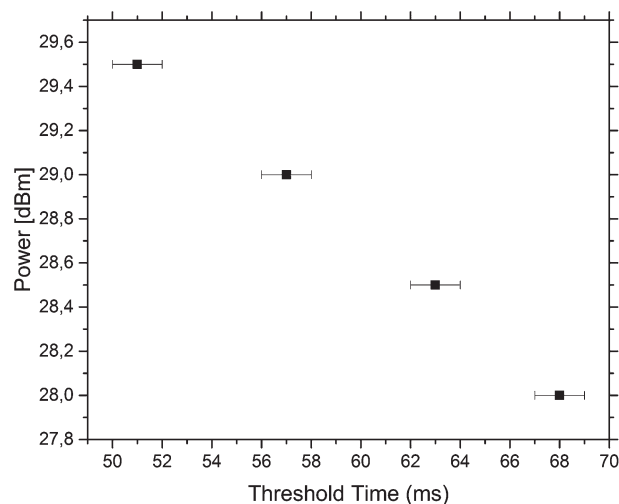
Fig. 5 Power and threshold pulse length needed to push out a droplet. The third trap, being the middle trap, was monitored to measure the minimum time needed to push out a trapped droplet. The threshold time needed to push out increased with the decreasing power of the SAW.

and cell sorting,[51–54] reorientation of nano-objects like carbon nanotubes[55] and liquid crystals,[56] pumping of fluids[57] and microcentrifugation.[58,59]

Here, the generated water droplets in oil, using a T-junction, are directed to the trapping system. The excited SAW propagating on the piezoelectric substrate hits the coupling channel. The position is controlled by the applied fre-

quency. At this location it generates a bubble,[60] possibly by heating up the oil.[61–68] The bubble grows, while acoustic energy is applied, over time and pushes the oil out of the coupling channels through the restrictions. After the SAW is switched off, the bubble collapses within several milliseconds, inducing a spontaneous high pressure gradient. Droplets are sucked into the traps and each trap is filled with one droplet each.

The traps have a height of 45 μm in contrast to the 30 μm main channel. The channels are 30 μm in width and height. The droplets generated pass through the channels in a squeezed state and when a droplet is sucked into a trap, it expands to a spherical shape and gets trapped. The Laplace pressure generated by deforming into a non-spherical shape hinders droplets from escaping the trap and makes the system more robust. The restrictions in the system have a height of 15 μm, increasing this pressure effect by deforming and guarantee that no droplet passes through a restriction.

The SAW is used to actuate droplets in individual traps. The tapered IDT is actuated at different positions, controlled by the applied frequency, to hit individual traps. The application of the SAW generates a bubble in the coupling channel at the specific location, which pushes the oil into the traps through the restrictions. This in turn pushes the droplet out of the trap. When the SAW is switched off, the bubble collapses and creates a pressure gradient that sucks another droplet into the same trap.

To achieve the actuation of individual droplets, the SAW is switched on in small pulses of 350 ms and a constant power of 29 dBm is used for all measurements. These values are chosen as this combination of power and pulse length works for the setup and all traps can be individually actuated. It should be noted that the third trap can be actuated individually with a much smaller pulse length of 57 ms at a power of 29 dBm but this pulse length cannot actuate all the traps individually. When the power is lowered, the pulse length needed to actuate a droplet increases. As the SAW, generating the bubble by the induced energy, couples into the channel far away from the droplets, potential contents in the drops, like cells, are not directly exposed to the acoustic field and the actuation is non-invasive. This makes this approach ideal for sensitive samples.

It is observed that a higher concentration of the surfactant, leading to a lower surface tension, decreases the robustness of the system. The trapped droplets are then able to squeeze through the restrictions as the Laplace pressure induced by deformation is less. A stable trapping is not possible at much higher surfactant concentrations. This observation is similar to the findings from earlier experiments with simpler channel designs using single-layer PDMS fabrication where a robust and reliable capture was not feasible either.

We have shown a robust system for the fast trapping and selective release of picoliter droplets on demand. This system with a rate of 460 drops per s demonstrates a fast trapping and release of individual droplets in 57 ms. It is for the first time that the controlled release and trapping of individual traps has

been demonstrated in a continuous high-speed flow. Most of the previous studies either relied on the surface charged trapping of droplets or trapped droplets randomly based on a probabilistic distribution. None of the existing systems work at high speed flow rates with high drop rates of over 400 drops per s. For other systems, the release of trapped droplets often relies on disrupting the continuous flow and reversing the flow of the continuous phase.

Some of the applications of the present system are obvious, as droplets could be loaded with various contents, including cells, then observed in the traps for a defined time and finally pushed out into the constant flow again. This is particularly useful for examining random samples in a running system. Importantly, the system offered robust and stable operation over a long time (half an hour or more), allowing the holding of the droplets in the observation field over user-defined intervals, even without switching off or altering the continuous flow. During observation we could not measure the shrinkage of drops due to water dissolving in the continuous oil phase or PDMS. However, for extremely long incubation times of several days as necessary for some cell assays, evaporation could be further reduced by applying a water saturated atmosphere as has been demonstrated before in droplet based fluidic systems.[69] The ability to manipulate the droplets in multiple traps makes it possible to compare the chemical processes taking place in two or more droplets containing different analytes. This feature could be used e.g. in a quality check at different times for a running experiment. Our approach is non-invasive and biocompatible since the drops are not exposed to acoustic fields directly but are stirred only by the flow and pressure differences caused by an acoustically formed bubble, far away from the droplet sample. Another major advantage of this system is that it is independent of the cargo of the droplets. The device we presented here is a versatile platform for droplet incubation and measurement for continuous fast flowing droplet systems that can simply be used in combination with other operations on the fluidic chip and can be integrated as an additional module of a fluidic chip (μTAS-chip) without interacting with other components on the chip nor interacting with the flow conditions. The acoustic trapping mechanism could be further developed for on-demand trapping of single droplets. This would provide a more controlled way for observing and measuring during a running experiment. If the selective readout of traps is combined with a more complex microfluidic channel design, the sorting of the observed droplets into another outlet is feasible. After trapping, the contents in droplets could be mixed via acoustic streaming induced by a SAW of a lower power and pulse length.[70] Also the acoustic merging of two droplets in a modified trap seems feasible in the near future.[25] The droplet trap has the potential for further multiplexing. Based on the design we have demonstrated here, the footprint of a single trap is about 0.15 mm^2. On a standard microscopic slide of 26 mm × 76 mm, therefore, about 10 000 traps could be integrated. These examples show the broad range of potential applications of this method, which we plan to explore next.

Conflicts of interest

There are no conflicts to declare.

Acknowledgements

References

1 S.-Y. Teh, R. Lin, L.-H. Hung and A. P. Lee, *Lab Chip*, 2008, **8**, 198–220.

2 P. S. Dittrich and A. Manz, *Nat. Rev. Drug Discovery*, 2006, **5**, 210–218.

3 B. Ziaie, *Adv. Drug Delivery Rev.*, 2004, **56**, 145–172.

4 J. J. Agresti, E. Antipov, A. R. Abate, K. Ahn, A. C. Rowat, J.-C. Baret, M. Marquez, A. M. Klibanov, A. D. Griffiths and D. A. Weitz, *Proc. Natl. Acad. Sci. U. S. A.*, 2010, **107**, 4004–4009.

5 M. T. Guo, A. Rotem, J. A. Heyman and D. A. Weitz, *Lab Chip*, 2012, **12**, 2146.

6 B. Zheng, L. S. Roach and R. F. Ismagilov, *J. Am. Chem. Soc.*, 2003, **125**, 11170–11171.

7 F. Dutka, A. S. Opalski and P. Garstecki, *Lab Chip*, 2016, **16**, 2044–2049.

8 T. S. Kaminski, O. Scheler and P. Garstecki, *Lab Chip*, 2016, **16**, 2168–2187.

9 M. A. Czekalska, T. S. Kaminski, S. Jakiela, K. Tanuj Sapra, H. Bayley and P. Garstecki, *Lab Chip*, 2015, **15**, 541–548.

10 P. M. Korczyk, L. Derzsi, S. Jakieła and P. Garstecki, *Lab Chip*, 2013, **13**, 4096.

11 V. van Steijn, P. M. Korczyk, L. Derzsi, A. R. Abate, D. A. Weitz and P. Garstecki, *Biomicrofluidics*, 2013, **7**, 24108.

12 L. Derzsi, T. S. Kaminski and P. Garstecki, *Lab Chip*, 2016, **16**, 893–901.

13 S. S. Bithi and S. A. Vanapalli, *Biomicrofluidics*, 2010, **4**, 44110.

14 H. Boukellal, S. Selimović, Y. Jia, G. Cristobal and S. Fraden, *Lab Chip*, 2009, **9**, 331–338.

15 A. Huebner, D. Bratton, G. Whyte, M. Yang, A. J. DeMello, C. Abell and F. Hollfelder, *Lab Chip*, 2009, **9**, 692–698.

16 H. Nuss, C. Chevallard, P. Guenoun and F. Malloggi, *Lab Chip*, 2012, **12**, 5257–5261.

17 C. H. J. Schmitz, A. C. Rowat, S. Köster and D. A. Weitz, *Lab Chip*, 2009, **9**, 44–49.

18 W. Shi, J. Qin, N. Ye and B. Lin, *Lab Chip*, 2008, **8**, 1432–1435.

19 M. Sun, S. S. Bithi and S. A. Vanapalli, *Lab Chip*, 2011, **11**, 3949–3952.

20 Q. Zhang, S. Zeng, J. Qin and B. Lin, *Electrophoresis*, 2009, **30**, 3181–3188.

21 S. S. Bithi and S. A. Vanapalli, *Soft Matter*, 2015, **11**, 5122–5132.

22 Y. Bai, X. He, D. Liu, S. N. Patil, D. Bratton, A. Huebner, F. Hollfelder, C. Abell and W. T. S. Huck, *Lab Chip*, 2010, **10**, 1281.

23 L. Schmid, D. A. Weitz and T. Franke, *Lab Chip*, 2014, **14**, 3710–3718.

24 D. J. Collins, T. Alan, K. Helmerson and A. Neild, *Lab Chip*, 2013, **13**, 3225–3231.

25 M. Sesen, T. Alan and A. Neild, *Lab Chip*, 2014, **14**, 3325–3333.

26 M. Sesen, T. Alan and A. Neild, *Lab Chip*, 2015, **15**, 3030–3038.

27 S. Li, X. Ding, F. Guo, Y. Chen, M. I. Lapsley, S.-C. S. Lin, L. Wang, J. P. McCoy, C. E. Cameron and T. J. Huang, *Anal. Chem.*, 2013, **85**, 5468–5474.

28 J. Nam, H. Lim, C. Kim, J. Yoon Kang and S. Shin, *Biomicrofluidics*, 2012, **6**, 24120–2412010.

29 C. Dammann and S. Köster, *Lab Chip*, 2014, **14**, 2681–2687.

30 L. Lin, Y.-S. Chu, J. P. Thiery, C. T. Lim and I. Rodriguez, *Lab Chip*, 2013, **13**, 714.

31 B. Ahn, K. Lee, H. Lee, R. Panchapakesan, L. Xu, J. Xu and K. W. Oh, *Lab Chip*, 2011, **11**, 3915.

32 X. Chen, S. Shojaei-Zadeh, M. L. Gilchrist and C. Maldarelli, *Lab Chip*, 2013, **13**, 3041.

33 A. Yamada, S. Lee, P. Bassereau and C. N. Baroud, *Soft Matter*, 2014, **10**, 5878.

34 P. Abbyad, R. Dangla, A. Alexandrou and C. N. Baroud, *Lab Chip*, 2011, **11**, 813–821.

35 T. Yeo, S. J. Tan, C. L. Lim, D. P. X. Lau, Y. W. Chua, S. S. Krisna, G. Iyer, G. S. Tan, T. K. H. Lim, D. S. W. Tan, W.-T. Lim and C. T. Lim, *Sci. Rep.*, 2016, **6**, 22076.

36 M. Sesen, C. Devendran, S. Malikides, T. Alan and A. Neild, *Lab Chip*, 2017, **17**, 438–447.

37 J. H. Jung, G. Destgeer, J. Park, H. Ahmed, K. Park and H. J. Sung, *Anal. Chem.*, 2017, **89**, 2211–2215.

38 W. Wang, C. Yang and C. M. Li, *Lab Chip*, 2009, **9**, 1504.

39 W. Wang, C. Yang, Y. Liu and C. M. Li, *Lab Chip*, 2010, **10**, 559.

40 G. Destgeer and H. J. Sung, *Lab Chip*, 2015, **15**, 2722–2738.

41 X. Ding, P. Li, S.-C. S. Lin, Z. S. Stratton, N. Nama, F. Guo, D. Slotcavage, X. Mao, J. Shi, F. Costanzo and T. J. Huang, *Lab Chip*, 2013, **13**, 3626–3649.

42 T. Dung Luong and N. Trung Nguyen, *Micro Nanosyst.*, 2010, **2**, 217–225.

43 T. Frommelt, M. Kostur, M. Wenzel-Schäfer, P. Talkner, P. Hänggi and A. Wixforth, *Phys. Rev. Lett.*, 2008, **100**, 1–4.

44 C. Y. Lee, C. L. Chang, Y. N. Wang and L. M. Fu, *Int. J. Mol. Sci.*, 2011, **12**, 3263–3287.

45 A. Wixforth, C. Strobl, C. Gauer, A. Toegl, J. Scriba and Z. v. Guttenberg, *Anal. Bioanal. Chem.*, 2004, **379**, 982–991.

46 T. Franke and A. Wixforth, *ChemPhysChem*, 2008, **9**, 2140–2156.

47 A. Renaudin, P. Tabourier, J.-C. Camart and C. Druon, *J. Appl. Phys.*, 2006, **100**, 116101.

48 A. Renaudin, P. Tabourier, V. Zhang, J. C. Camart and C. Druon, *Sens. Actuators, B*, 2006, **113**, 389–397.

49 M. Tan, J. Friend and L. Yeo, *Phys. Rev. Lett.*, 2009, **103**, 24501.

50 A. Winkler, S. M. Harazim, S. B. Menzel and H. Schmidt, *Lab Chip*, 2015, **15**, 3793–3799.

51 T. Franke, S. Braunmüller, L. Schmid, A. Wixforth and D. A. Weitz, *Lab Chip*, 2010, **10**, 789.

52 V. Skowronek, R. W. Rambach, L. Schmid, K. Haase and T. Franke, *Anal. Chem.*, 2013, **85**, 9955–9959.

53 R. W. Rambach, V. Skowronek and T. Franke, *RSC Adv.*, 2014, **4**, 60534–60542.

54 V. Skowronek, R. W. Rambach and T. Franke, *Microfluid. Nanofluid.*, 2015, **19**, 335–341.

55 C. J. Strobl, C. Schaeflein, U. Beierlein, J. Ebbecke and A. Wixforth, *Appl. Phys. Lett.*, 2004, **85**, 1427.

56 Y. J. Liu, X. Ding, S. C. S. Lin, J. Shi, I. K. Chiang and T. J. Huang, *Adv. Mater.*, 2011, **23**, 1656–1659.

57 X. Y. Du, Y. Q. Fu, J. K. Luo, A. J. Flewitt and W. I. Milne, *J. Appl. Phys.*, 2009, **105**, 24508.

58 R. V. Raghavan, J. R. Friend and L. Y. Yeo, *Microfluid. Nanofluid.*, 2010, **8**, 73–84.

59 H. Li, J. R. Friend and L. Y. Yeo, *Biomed. Microdevices*, 2007, **9**, 647–656.

60 T. Lee, J. G. Ok, H. S. Youn and L. J. Guo, in IEEE Int. Ultrason. Symp. Proc., 2014, pp. 1041–1044.

61 D. Beyssen, L. Le Brizoual, O. Elmazria, P. Alnot, I. Perry and D. Maillet, in 2006 IEEE Ultrasonics Symposium, IEEE, 2006, vol. 1, pp. 949–952.

62 J. Kondoh, N. Shimizu, Y. Matsui, M. Sugimoto and S. Shiokawa, in IEEE Ultrasonics Symposium, 2005, IEEE, 2005, vol. 2, pp. 1023–1027.

63 W. Tseng, J. Lin, W. Sung, S.-H. Chen and G.-B. Lee, *J. Micromech. Microeng.*, 2006, **16**, 539–548.

64 J. Kondoh, N. Shimizu, Y. Matsui, M. Sugimoto and S. Shiokawa, *Sens. Actuators, A*, 2009, **149**, 292–297.

65 J. K. Luo, Y. Q. Fu and W. I. Milne, in *Modeling and Measurement Methods for Acoustic Waves and for Acoustic Microdevices*, ed. M. G. Beghi, InTech, 2013, pp. 515–556.

66 Z. Yang, S. Matsumoto, H. Goto, M. Matsumoto and R. Maeda, *Sens. Actuators, A*, 2001, **93**, 266–272.

67 T. Luong, V. Phan and N.-T. Nguyen, *Microfluid. Nanofluid.*, 2011, **10**, 619–625.

68 B. H. Ha, K. S. Lee, G. Destgeer, J. Park, J. S. Choung, J. H. Jung, J. H. Shin and H. J. Sung, *Sci. Rep.*, 2015, **5**, 11851.

69 S. Köster, F. E. Angilè, H. Duan, J. J. Agresti, A. Wintner, C. Schmitz, A. C. Rowat, C. A. Merten, D. Pisignano, A. D. Griffiths and D. A. Weitz, *Lab Chip*, 2008, **8**, 1110.

70 J. Reboud, Y. Bourquin, R. Wilson, G. S. Pall, M. Jiwaji, A. R. Pitt, A. Graham, A. P. Waters and J. M. Cooper, *Proc. Natl. Acad. Sci. U. S. A.*, 2012, **109**, 15162–15167.